Carbohydrate Polymers 101 (2014) 1166–1175

Contents lists available at ScienceDirect

Carbohydrate Polymers

journal homepage: www.elsevier.com/locate/carbpol

Preparation and characterization of SiO_2/CMC/Ag hybrids with antibacterial properties

Nadezhda Rangelova[a,*], Lyubomir Aleksandrov[b], Tsvetelina Angelova[c], Nelly Georgieva[c], Rudolf Müller[d]

[a] University of Chemical Technology and Metallurgy, Department of Fundamentals of Chemical Technology, str. bld. 8 Kl. Ohridski, 1756 Sofia, Bulgaria
[b] Institute of General and Inorganic Chemistry, Bulgarian Academy of Sciences, Acad. G. Bonchev str. bl. 11, 1113 Sofia, Bulgaria
[c] University of Chemical Technology and Metallurgy, Department of Biotechnology, str. bld. 8 Kl. Ohridski, 1756 Sofia, Bulgaria
[d] Hamburg University of Technology, Institute of Technical Biocatalysis, Denicke str. 15, 21071 Hamburg, Germany

ARTICLE INFO

Article history:
Received 27 June 2013
Received in revised form 5 October 2013
Accepted 12 October 2013
Available online 23 October 2013

Keywords:
Sol–gel method
Carboxymethyl cellulose
Silver nanoparticles
Antibacterial activity

ABSTRACT

Amorphous hybrids based on sodium salt of carboxymethyl cellulose (CMC) and tetraethoxysilane (TEOS) containing silver nanoparticles were prepared by sol–gel method. The amorphous structure, morphology and antibacterial behavior were clarified. The thermal stability of obtained hybrids decreased with the increase in silver content from 0.5 to 1.5 wt%. Infrared spectra of the material suggest that the main interaction between the cellulose ether and silica network is via hydrogen bonds (bands at ~3540 and 3625 cm^{-1}). According to UV–vis spectra the silver is present in two different states Ag^+ (absorption band at ~210 nm) and Ag^0 (band at ~300 nm). The different sizes of silver particles are present as clusters. It was demonstrated that these hybrids have a well pronounced antibacterial activity against *B. subtilis* and *E. coli* K12. Even the hybrid with 0.5 wt% Ag has efficient antibacterial activity for both Gram-positive and Gram-negative bacteria.

1. Introduction

Preparation of nano-sized silver (AgNPs) based materials are amongst the most emerging areas in the field of nanotechnology. Nano dimension materials become important because their unique applications include solar energy conversion, photonics, catalysis, microelectronics, antimicrobial functionalities, and water treatment (Amin, Anwar, Janjua, Iqbal, & Rashid, 2012; Dastjerdi, Montazer, & Shahsavan, 2010; Du, Niu, Xu, Xu, & Fan, 2009; Savage & Diallo, 2005; Setua et al., 2007; Yugang, Mayers, & Xia, 2003). A variety of methods exists to synthesize AgNPs, including the microemulsion technique, γ-ray, UV or microwave irradiation, spray pyrolysis and sol–gel (Ahmad, Shameli, Darroudi, Yunus, & Ibrahim, 2009; Angelova, Rangelova, Yuryev, Georgieva, & Müller, 2012; García-Barrasa, López-de-Luzuriaga, & Monge, 2011; Husein & Nassar, 2008; Kim, Lee, & Kim, 2006; Rangelova, Nenkova, Radev, Samuneva, & Aleksiev, 2007; Sharma, Yngard, & Lin, 2009;Vasireddy, Paul, & Mitra, 2012). Chemical reduction is the most frequently applied method for the preparation of silver nanoparticles as stable, colloidal dispersions in water or organic solvents (Khan, Al-Thabaiti, Obaid, & Al-Youbi, 2011; Kheybari, Samadi, Hosseini, Fazeli, & Fazeli, 2010; Sharma et al., 2009; Shi et al., 2011; Tao, Sinsermsuksaku, & Yang, 2006; Wiley, Sun, Mayers, & Xi, 2005). Initially, the reduction of various complexes with Ag^+ ions leads to the formation of silver atoms (Ag^0), which is followed by agglomeration into oligomeric clusters. These clusters can lead to the formation of colloidal Ag particles (Kapoor, Lawless, Kennepohl, Meisel, & Serpone, 1994). The green synthetic methods using natural polymers have shown a great potential in AgNP synthesis. Natural polymers, such as cellulose and its derivatives, alginates, starch, dextran, guar gums, gelatin and others (Abdel-Halim & Al-Deyab, 2011; Abdel-Mohsen et al., 2012; Bankura et al., 2012; Li et al., 2011a, 2011b; Lin et al., 2013; Maity et al., 2012; Moura, de Mattoso, & Zucolotto, 2012; Pandey, Goswami, & Nanda, 2012; Pourjavadi & Soleyman, 2011; Singh & Ahmed, 2012a; Vasireddy et al., 2012; Yang, Xie, Deng, Bian, & Hong, 2012) have been used as matrices or stabilizers for the preparation of metallic nanoparticles because of their non-toxicity and biocompatibility. The biopolymers usually have abundant hydroxyl or carboxyl groups in their polymer backbone. The mechanism of silver interaction with functional groups of biopolymers follows next steps. The presence of large amount of polar —OH groups in biopolymers have the ability to coordinate silver ions. When the hydroxyl groups and silver ions form coordination bonds, the interactions among the resultant Ag particles and the oxygen atoms of —OH groups become stronger (Abdel-Halim & Al-Deyab, 2011; Bankura et al., 2012; Pandey et al., 2012). On the other hand the presence of negative charged carboxylic groups (COO^-) in the polymer

* Corresponding author. Tel.: +359 2 8163 307.
E-mail address: rangelovang@gmail.com (N. Rangelova).

0144-8617/$ – see front matter © 2013 Elsevier Ltd. All rights reserved.
http://dx.doi.org/10.1016/j.carbpol.2013.10.041

backbone and positive charged of Ag ions lead to electrostatic interaction (Abdel-Mohsen et al., 2012; Hebeish, El-Rafie, Abdel-Mohdy, Abdel-Halim, & Emam, 2010). According to Juby et al. (2012) the presence of —COOH and —OH groups in the polymeric chains lead to the formation of weak intermolecular cross-links between the polymer chains, restricting their mobility.

Sodium carboxymethyl cellulose (CMC) is a water soluble polymer derived from natural cellulose (Feller & Wilt, 1990; Hatakeyama & Hatakeyama, 2004; Jiang et al., 2011). This polymer is biocompatible and biodegradable. It is, therefore, often used in the biomedical field (Chang, Duan, Cai, & Zhang, 2010; Feller & Wilt, 1990). It has been routinely used for many years now as a food additive to give the food smoothness, as thickener, as phase and emulsion stabilizer, as suspending agent and in other applications (Feller & Wilt, 1990; Kim, 2007). As mentioned above CMC like natural polymers have been used for "green" synthesis of AgNps. In all cases cellulose ether acts as both a reducing and a stabilizing agent in the reaction (Chen, Wang, Zhang, & Jin, 2008; Hebeish et al., 2010; Hebeish, Hashem, El-Hady, & Sharaf, 2013). CMC hydrogels loaded with AgNPs are materials with potential applications in textile or medical fields.

Many hybrids have been prepared from silica precursors/biopolymer mixed solutions by a sol–gel method. Sol–gel derived silica hybrid materials have many attractive applications as adsorption of enzymes and metal ions, good mechanical properties, thermal stability, and resistance against microbial attack and organic solvents. Tetramethoxysilane (TMOS) and TEOS are common precursors that are currently applied to obtain hybrid materials. TEOS is of considerable current use on an industrial scale owing to several advantages over other silica precursors. When brought into contact with water, the TEOS is hydrolyzed and its products are involved in polycondensation reaction that yield hydrated SiO_2 (Kickelbick, 2007; Shchipunov, 2008).

Up to now only a few publication showing the synthesis and structure of CMC/SiO_2 hybrid materials obtained with or without silver exist in the literature. Reactive octa-aminopropyl polyhedral oligomeric silsesquioxane (POSS–NH_2) and CMC have been used as starting materials. The mechanism for preparation of novel POSS/CMC hybrid hydrogel has been described by the aggregation of POSS–NH_2 nanoparticles and the formation of POSS–CMC hybrid block copolymers, which was driven by the hydrogen bonding interactions between the amino groups of POSS–NH_2 and the carboxyl groups of CMC. The obtained hybrids had specific properties such as good mechanical strength, high adsorption capacity for water and dyes. They offer potential applications in drug release systems, food, cosmetic and water purification (Liu et al., 2013). Benmouhoub, Simmonet, Agoudjil, & Coradin (2008) synthesized silica/carboxymethyl-cellulose hybrid gels using aqueous silicates as promising alternative precursors to SiO_2 alkoxides for the development of a greener sol–gel process. The authors suggested that the hydrogen bond formation, a key mode of interaction in biological systems and in aqueous chemistry, appears to be responsible for the polymer/silica association. CMC–AgNp–SiO_2 hybrids have been synthesized by sol–gel process in the presence of an alkali catalyst. TMOS was used as silica precursor. The hybrid synthesis was optimized to obtain an efficient matrix for amylase immobilization (Singh & Ahmed, 2012b).

In our previous investigations we reported for successfully preparation of silica/biopolymers/silver hybrid materials by sol–gel method (Angelova et al., 2012; Rangelova et al., 2007; Rangelova, Georgieva, Mileva, Yuryev, & Müller, 2012). Hybrid materials using SiO_2 precursors such as TEOS, TMOS and low methoxyl pectin was obtained. The different size and shape of silver nanoparticles was presented on the matrix surface (Rangelova et al., 2007). Silica hybrid materials containing TEOS and hydroxypropyl cellulose with incorporation of silver were prepared and their structure, surface morphology, and antibacterial activity were examined. The homogeneity of distribution of the silver particles was determined additionally and they demonstrated good bactericidal activity (Angelova et al., 2012). In other work we represented the new generation of sol–gel antibacterial silica hybrid materials based on ethyl trimethoxysilane (ETMS), CMC and silver. In this case used silica precursor does not allow the homogeneity distribution and irregular shape of silver nanoparticles (Rangelova et al., 2012).

These results and above-mentioned literature data motivate us to check the possibility to combine the green method (using CMC as non-toxic reducer and stabilizer) and the sol–gel approach (using TEOS as SiO_2 source) for successful synthesis of hybrid materials. We also examined the structure and antibacterial behavior of SiO_2/CMC hybrids containing different amount of silver.

2. Materials and methods

2.1. Materials

The sodium salt of carboxymethyl cellulose, tetraethoxysilane and silver nitrate ($AgNO_3$) were purchased from Aldrich and nitric acid from Merck. They were used without further purification.

2.2. Preparation of SiO_2/CMC/Ag hybrid materials

The sol–gel synthesis of SiO_2/CMC hybrids with or without silver was carried out by a multi-step method using acid hydrolysis reaction (Scheme 1). The quantities necessary to obtain hybrids with 10 wt% cellulose derivative and silver content are calculated to SiO_2 assuming that the precursor (TEOS) is completely hydrolyzed.

Step 1: Dissolving of CMC: 10 wt% of cellulose ether was dissolved in 10 mL hot water on a magnetic stirrer to produce *Sol A.*

Step 2: Pre-hydrolyzation of silica source: TEOS (5 mL) was used as SiO_2 precursor to generate the siloxane network in the hybrids. It was pre-hydrolyzed with water (1.5 mL) and 0.1 N HNO_3 (1.5 mL) solutions as catalyst (*Sol B*). The obtained sols were homogenized on magnetic stirrer for 1 h to produce totally clear solutions.

Step 3: Dissolving of $AgNO_3$: Different amounts of $AgNO_3$ were used to produce hybrids with silver content 0.0 wt%, 0.5 wt%, 1.0 wt% and 1.5 wt% Ag. Silver nitrate was slowly added to the above-mentioned solution (*Sol B*). The formed suspension was stirred until complete dissolution of $AgNO_3$.

Step 4: Preparation of mixed *Sol C*: After dissolving the silver salt, Sol A was mixed with Sol B under stirring and homogenization for 40–60 min.

The obtained *Sols C* were kept at 50 °C for gelation, aging and drying. The newly synthesized hybrids were tested as antibacterial materials against Gram-positive and Gram-negative bacteria.

2.3. Sample characterization

2.3.1. X-ray diffraction (XRD)

X-ray diffraction patterns were used to investigate the crystallinity of the materials. For the XRD measurements a Bruker D8 Advance diffractometer was used at Cu $K\alpha$ radiation in $10 < 2\theta < 80$ range.

2.3.2. Fourier transform infrared (FT-IR) spectroscopy

The structural building units of obtained hybrid materials were determined by FT-IR spectra using KBr pellet technique on a Bruker's VERTEX 70 spectrometer with a resolution of $\pm 1\,cm^{-1}$, by collecting 32 scans in the range 4000–400 cm^{-1}.

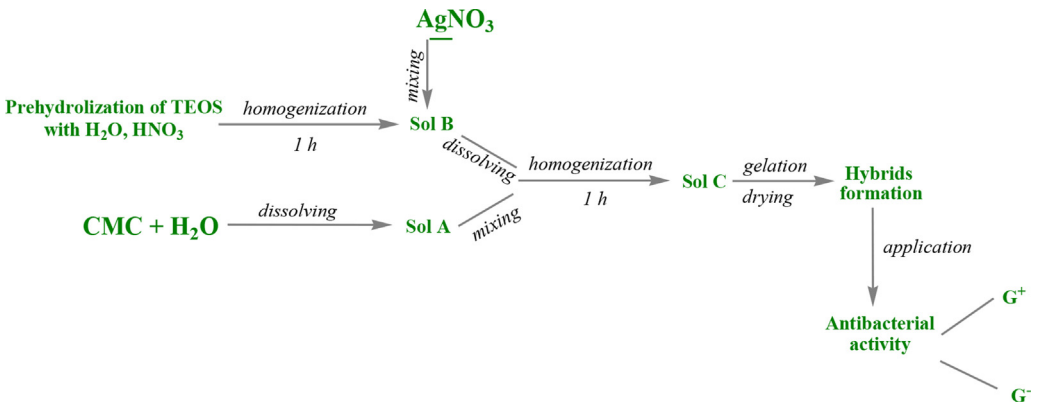

Scheme 1. Synthesis and application of SiO_2/CMC/Ag hybrid materials.

2.3.3. Scanning and transmission electron microscopy

Scanning electron microscopy (SEM) was employed to study the morphology of the obtained hybrids. SEM images were taken with a Microscope LEO 1530, Gemini. The obtained materials were covered with gold using BAL-TEC/SCD 050 Sputter coater. Energy-dispersive X-ray spectroscopy (EDS) was used to determine the elements on sample surfaces. Transmission electron microscopy (TEM) and high resolution transmission electron microscopy (HRTEM) were used to determine the size of silver nano-particles inside the hybrids. The TEM investigations were performed on a TEM JEOL 2100 instrument at accelerating voltage of 200 kV. The specimens were prepared by grinding and dispersing the powders in ethanol by ultrasonic treatment for 6 min. The suspensions were dripped on standard carbon/Cu grids.

2.3.4. Ultraviolet and visible (UV–vis) spectroscopy

The optical absorption spectra in the ultraviolet and visible region were investigated by Spectrophotometer Evolution 300 in the wavelength range 200–1100 nm. The absorbance test was performed on the powdered samples. The absorption spectra were converted from the refraction by Kubelka–Munk method.

2.3.5. Differential thermal analysis (DTA/TG)

The thermal stability of synthesized amorphous hybrids was determinated by DTA/TG analysis. A Seteram Labsysis Evo 1600 instrument was used for recording of thermo diagrams over the range from room temperature up to 700 °C. The heating rate was 10°/min in air atmosphere under an air flow of 20 mL/min in order to determine the released gas phases during the increase of temperature by the mass spectrometer OminStar Preffer vacuum.

2.4. Antibacterial activity studies

The antibacterial effect of obtained hybrid materials was tested against aerobic Gram-positive *Bacillus subtilis* and facultative anaerobic Gram-negative *Escherichia coli* K12. The strains were obtained from the University of Hamburg–Harburg teaching laboratory and were cultured on LB agar plates for 18 h at 37 °C before use.

2.4.1. Determination of antibacterial activity in LB broth measuring turbidity

A single colony of *B. subtilis* and *E. coli* K 12 respectively was used for inoculating 50 mL liquid LB medium. 10 mg from the newly obtained hybrid materials with different silver contents (from 0.5 to 1.5 wt%) were placed in a flask with the investigated strains. The positive control contained bacteria and hybrid materials without silver. The cultivation process was performed on a rotary shaker (200 rpm) at 30 °C (*B. subtilis*) and 37 °C (*E. coli* K 12) for 24 h. Aliquots were taken every hour and optical density was measured at 620 nm.

2.4.2. Antibacterial activity based on LB agar plating

Bacterial growth inhibitory effect of hybrid materials was further confirmed by plating on LB agar plates. 200 μL of bacterial broth suspension after 24 h of strains cultivation in the presence of hybrid materials with different silver content were seeded on LB agar plates. Samples containing bacteria and hybrid materials without Ag were plated as positive controls. The plates were incubated 24 h at 30 °C for *B. subtilis* and 37 °C for *E. coli* K 12 followed by counting the number of colonies on the plate. The measurement of antibacterial activity of hybrid materials was calculated according to Rivero et al. (2011), between the control sample and the test sample.

$$Cell\ \ reduction\ \ (\%) = \left(1 - \frac{Test\ sample\ \left(\frac{CFU}{mL}\right)}{Control\ \left(\frac{CFU}{mL}\right)}\right) \times 100$$

3. Results and discussion

Homogeneous amorphous hybrids based on the sodium salt of carboxymethyl cellulose (CMC) and TEOS containing silver nanoparticles were obtained using sol–gel and green methods. In this method the biopolymer is used as a material for synthesis of new hybrids, as a reducing agent for silver ions and as a non-toxic material for stabilization of nanoparticles. The advantages of the green process are: there is no need to use reducing agents; the process can be conducted at ambient temperature and it is a rapid and environmentally friendly process (García-Barrasa et al., 2011; Sharma et al., 2009).

The XRD patterns of pure CMC and hybrid materials are shown in Fig. 1. The diffractogram of the cellulose derivative shows that, like all other natural polymers, it has a partially crystalline nature (Ghaffari, Navaee, Oskoui, Bayati, & Rafiee-Tehrani, 2007; Rangelova et al., 2011; Wang & Xu, 2006). Differences between cellulose ether and hybrid materials can be observed in the X-ray diffractograms shown in Fig. 1a and b, respectively. The shifting of the peak at $2\theta = 20°$ (CMC) to 24° (SiO_2/CMC hybrid) can be explained by rearrangement in the morphology of the polymeric chain after interaction between CMC and silica. Disappearance of the peak at ~37° in the hybrid (Fig. 1a) compared with the diffractogram of cellulose ether indicate successful incorporation of CMC molecules into the silica network (Yano, 1994).

The diffraction band at around 23° is characteristic of amorphous silica (Arreche, Blanco, Martín Martínez, & Vázquez, 2012; Li,

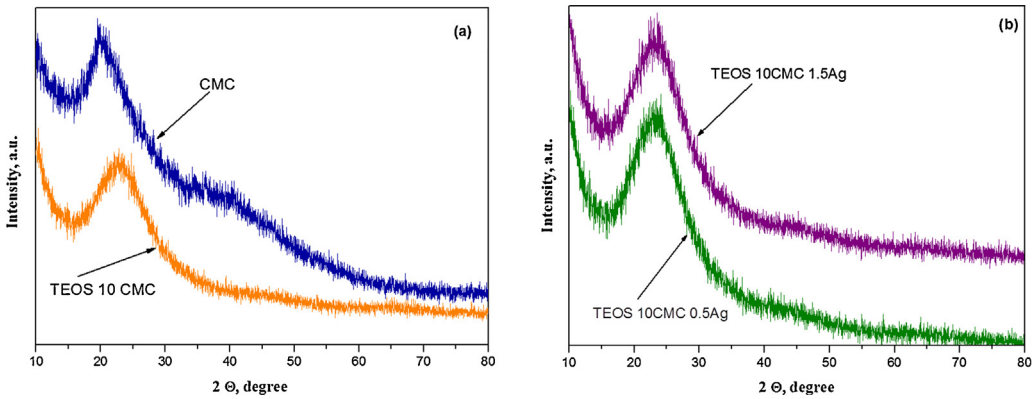

Fig. 1. XRD patterns of CMC and pure hybrid (a) and hybrids doped with different silver content (b).

Shi, & Guo, 2010; Zhang, Wu, He, & Yang, 2007). Similar diffraction patterns have been observed (Fig. 1). It can be seen that the diffraction patterns show slight shifting of "humps" at different angles center (2θ). It is clear that the hybrids remain amorphous. Moreover the decrease of diffraction peak intensities and the increased background noise present a sign that the crystalline structure of cellulose derivative has also been transformed to a less ordered state with its dissolution, recrystallization and incorporation into the composite structure. The absence of silver diffraction peaks in the samples can be explained with the overlap of a very broad peak of silica with the silver peaks, which are present in too small trace amounts to be detected by XRD (Singh & Ahmed, 2012a, 2012b).

The FTIR spectra of pure CMC and hybrid materials are compared to the spectra of hybrids doped with different amounts of silver in Fig. 2. The CMC spectrum (Fig. 2a) shows three frequency regions: from 3700 to 3100 cm^{-1}, 3000 to 2800 cm^{-1} and 1800 to 700 cm^{-1}.

In the first interval (3700–3100 cm^{-1}), the large absorption band can be assigned to the stretching vibrations of the hydroxyl groups. In this area OH groups can be divided into free (unsubstituted) hydroxyl groups and hydrogen bonding OH groups (Ibrahim, Koschella, Kadry, & Heinze, 2013; Li, Sun, & Wu, 2009; Li et al., 2011a,b; Wang & Somasundaran, 2005). On the other hand the hydrogen bonds of carboxymethyl cellulose macromolecule can be classify as interchain and intrachain hydrogen bonds (3380–3200 cm^{-1}) (Li et al., 2009). The bands at ~2920 and 2870 cm^{-1} correspond to asymmetric and symmetric C—H stretching vibrations of $-CH_2$ groups. The last interval (1800–700 cm^{-1}) is known as "fingerprint region", where the strong peak at around 1590 cm^{-1} is assigned to the non-hydrated C=O groups (Li et al., 2009; Rangelova et al., 2012; Yang, Li, He, Ren, & Wang, 2009). The bands in the range1350–1450 cm^{-1} represent deformation and valence vibrations of the C—OH bonds in the pyranoid ring. The stretching vibrations of the skeletal (C—O—C and C—C) glycosides linkages, as well as primary alcohol groups are found in the range between1078 and 1030 cm^{-1} (Ibrahim et al., 2013).

The FTIR spectra of pure hybrid material (Fig. 2a) and the spectra of hybrids doped with different silver content (Fig. 2b) are similar with the exception of the shoulder at around 1370 cm^{-1} due to NO_3^- groups (Jeon, Yi, & Oh, 2003). The bands in the range from 3200 to 3600 cm^{-1} can be attributed to silanol groups (Si—OH) or to absorbed water on the surface (Han, Taylor, Mantle, & Knowles, 2007; Rangelova et al., 2007, 2010, 2011, 2012). The bands at 1630 cm^{-1} can be assigned to the vibration of absorbed water. The characteristic bands of the silica network are usually found in the area from 1300 to 600 cm^{-1}.The bands at ~1080 cm^{-1} and 790 cm^{-1} can be assigned to the asymmetric and symmetric vibrations of the siloxane linkage (Si—O—Si) in the [SiO_4] tetraedra (Han et al., 2007; Kim et al., 2009; Nenkova, Radev, Rangelova, Aleksiev, & Samuneva, 2007; Rangelova et al., 2007, 2011). The bands at 950 cm^{-1} can be attributed to Si—OH groups (Han et al., 2007; Kim et al., 2009; Nenkova et al., 2007).

The main differences in the IR spectra (Fig. 2a and b) were observed in the range 3200–3600 cm^{-1}. The vibration of silanol groups which are associated with molecular water through H-bonds can be found above 3500 cm^{-1} (Kim et al., 2009). Many authors reported that the bands above 3500 cm^{-1} can be attributed to the vibration of hydrogen bonds formed between the biopolymer and the silica network (Han et al., 2007; Kim et al., 2009). It can be

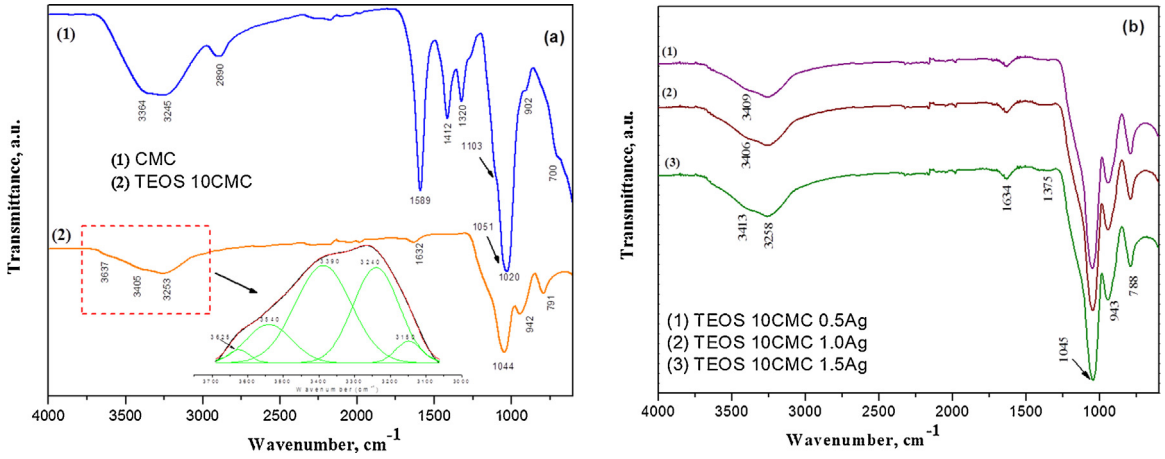

Fig. 2. IR spectra of CMC, pure hybrid (a) and hybrids doped with different silver content (b).

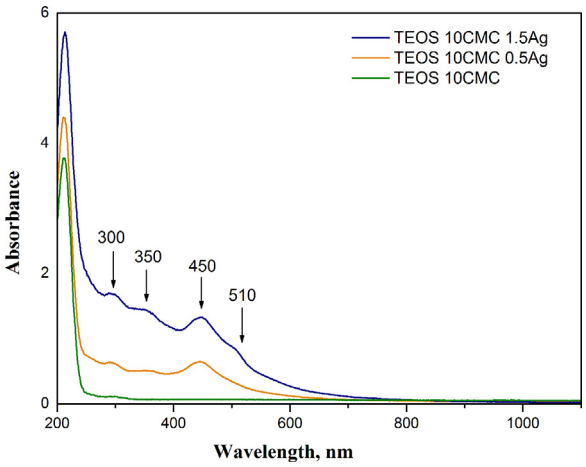

Fig. 3. UV–vis absorption spectra of pure hybrid and hybrids doped with different silver content.

seen that the broad band at around 3250 cm^{-1} becomes asymmetric with shoulders at ~3450 and 3640 cm^{-1} in the spectra of hybrid materials (Fig. 2b) and intensity decreases probably due to the formation of hydrogen bonding between CMC macromolecules and the SiO_2 network (Nenkova et al., 2007; Rangelova, 2012). For more details we decompose the peak in the region 3000–3800 cm^{-1}, where the spectra were fitted with a sum of Gaussian curves by means of least square method. The spectrum was decomposed into five components with a good fitting quality, giving the peaks at 3150, 3240, 3390, 3540 and 3625 cm^{-1}. The results indicate that the interactions between the biopolymer and silica network are bonded with H-bonds (3540 and 3625 cm^{-1}) (Nenkova et al., 2007; Rangelova, 2012). Mohan, Raju, Sambasivudu, Singh, & Sreedhar (2007) suggest that in the presence of silver ions in the hybrids the oxygen atoms of —OH and COOH groups get associated with silver clusters. This leads to broadening and shifting of stretching vibration of OH groups from 3260 to 3240 cm^{-1} between silver unloaded and silver loaded spectra (Juby et al., 2012).

It is well known that by UV–vis spectra useful structure information about the size and oxidation state of silver particles can be obtained. Fig. 3 presents the UV–vis absorption spectra of pure hybrid and hybrids doped with different amounts of silver ions (0.5 and 1.5 wt% Ag). Broad peaks were observed at ~300, 350, 440 nm for materials containing silver. It is noted that the presence, shape and peak position in these spectra correlates to the Ag content. Generally absorption bands in the region 200–250 nm correspond to the presence of Ag^+ ions and bands in the range 250–300 nm can be found with Ag^0 ions (Baia & Simon, 2007; Vulpoi, 2011). On the other hand it is well known that the absorption bands ~420 nm can be attributed to the surface plasmon resonance (Aziz, Abidin, & Arof, 2010; Baia & Simon, 2007; Silvert, Herrera-Urbina, & Tekaia-Elhsissen, 1997; Vulpoi, 2011). The absorption bands located at ~210 nm are present in all investigated hybrid materials including the initial amorphous matrix without Ag, where the maximum appears at 210 nm. As has been mentioned above, the Ag^+ signature can be seen in the region between 200 and 250 nm and analysis to assign this peak is a complicate. However, basically this signal comes from the initial matrix with absorption age $\lambda \approx 230$ nm and optical band gap $E_g \approx 5.39$ eV but a shift of the maximum value of this peak from 210 to 213 nm can be assigned to the presence of small amounts of Ag^+. It can be seen that in the UV–vis spectra of pure hybrid has no other absorption peaks. This means that the bands at ~300, 350, 440 nm can be attributed to the presence of silver in the amorphous matrix. The absorption peak at 300 nm can be attributed to the electronic transition of Ag^0. It has been reported that polymers which contain hydroxyl and carboxyl groups are responsible for Ag^+ reduction (Aziz et al., 2010; Silvert et al., 1997). Silvert et al. (1997) give an interpretation of this phenomenon with strong affinity of nitrogen and oxygen atoms of polar groups for silver ion and metallic silver.

The plasmon bands at ~440 nm can be related to the formation of silver nanoparticles and their concentration. It was established that with the increase of the silver content in the amorphous matrix the color changes from light brown to dark brown. The same results were reported from many authors (Aziz et al., 2010; Kang et al., 2004). Aziz et al. (2010) reported that the color of metal nanoparticles depends on the shape and size of the nanoparticles and only free electrons possess plasmon resonance in the visible spectra giving intense color.

The presence of an absorption signal at around 350 nm, a shoulder at 500 nm, which is typical for hybrid material containing 1.5 wt% Ag, can be explained by the presence of different sizes of silver nanoparticles. It was discussed that the absorption peaks at 420–430 nm are caused by silver nanoparticles with higher sizes than the particles giving a signal at 330–350 nm (Vulpoi, 2011). In this connection it maybe concluded that the silver nanoparticles in the obtained materials have different sizes and formed clusters.

The DTA curve of pure CMC (Fig. 4a) in the range from room temperature to 700 °C there are three exothermic effects that can be attributed to the depolymerization and subsequent combustion of cellulose ether (Singh & Ahmed, 2012b; Teotia, 2012; Zakharov, Ezhova, Koval, Kalinnikov, & Chalykh, 2005). The thermal analysis of the hybrid obtained without silver showed that it is extremely stable (even at 700 °C) as there were no exo-effects. The observed exothermic peaks at lower temperatures in DTA curves of hybrids with 0.5 and 1.5 wt% silver could be explained by degradation of complexes between silver and macromolecules of the cellulose derivative. In this way part of —OH and —COOH groups are blocked, which means that they are not free and cannot participate in the formation of H-bonds with the silica network.

Fig. 4b presents the spectra of the released gas phases when CMC, pure hybrid and hybrids doped with different silver content were heated. Comparing the curves of DTA analysis of cellulose ether (Fig. 4a) and data from gas spectroscopy of CO_2 (Fig. 4c) there is similarity between them. This confirms that a greater degree of phase transitions occur mainly by the release of CO_2 due to decomposition and combustion of CMC.

The TG curves of the thermal treatment of the samples are presented in Fig. 4d. They show that CMC undergoes mass loss of ~70%. On the other hand, the hybrid prepared without silvers show a weight loss only 3% which occur in the temperature range 50–150 °C and can be attributed to the water evaporation. For the hybrids doped with silver weight losses are in the range 8–17%, depending on the quantities of the included silver. As noted above, these losses can be attributed to the degradation of linkages between the silver and CMC macromolecules (Juby et al., 2012; Singh & Ahmed, 2012b).

Fig. 5 presents SEM images of the obtained hybrids. It can be seen that the hybrid without silver (Fig. 5a) has a smooth surface with wavy character and spherical inclusions (sodium particles) evenly distributed on the sample surface. The formed micro heterogeneities have an average size of ~0.9 μm. On the surface of the hybrid with 0.5 wt% Ag spherical particles with an average size in the range 30–100 nm can be seen, uniformly distributed in the amorphous matrix. The silver particles formed oval shaped clusters, which were evenly distributed. With the increase of the silver content to 1.5 wt% the formation of multiple clusters with an average diameter 0.5 μm can be seen. The EDS analysis demonstrates that the identified elements are O, C, Na, Ag, Si and Au, which are characteristic for the obtained materials.

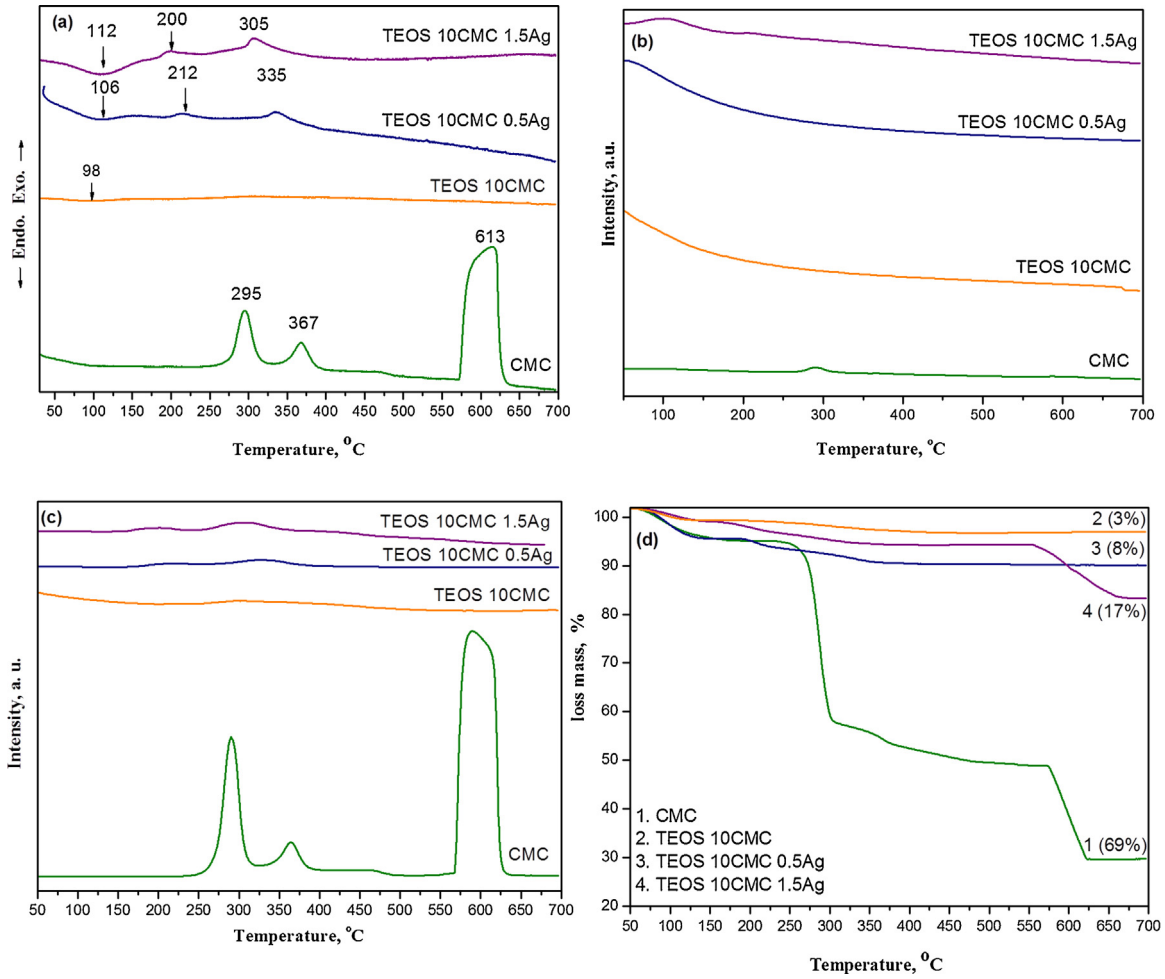

Fig. 4. Thermal parameters of CMC, pure hybrid and hybrids doped with different silver contents: DTA curves (a), realized as gas products H_2O (b) and CO_2 (c) during the thermal treatment, and TG curves (d).

To demonstrate the shape and size of the silver nano-particles within the obtained hybrids and to confirm the data from UV–vis spectroscopy TEM analysis were carried out. Fig. 6 presents TEM and HRTEM images of the obtained hybrid materials with different silver contents. In the micrographs the silver nanoparticles (dark part) with different shapes and sizes between 5 and 10 nm can be seen. Silver particles in the sample containing 1.5 wt% (Fig. 6c and d) are smaller than the particles in the sample containing 0.5 wt%

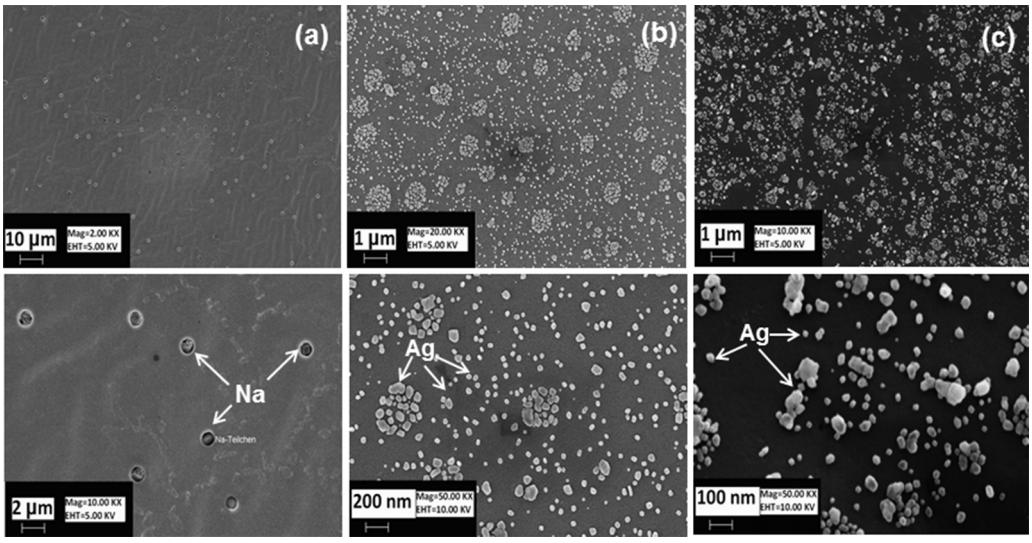

Fig. 5. SEM images of CMC/SiO_2 hybrid (a) and hybrids doped with different silver contents – 0.5 wt% (b) and 1.5 wt% (c).

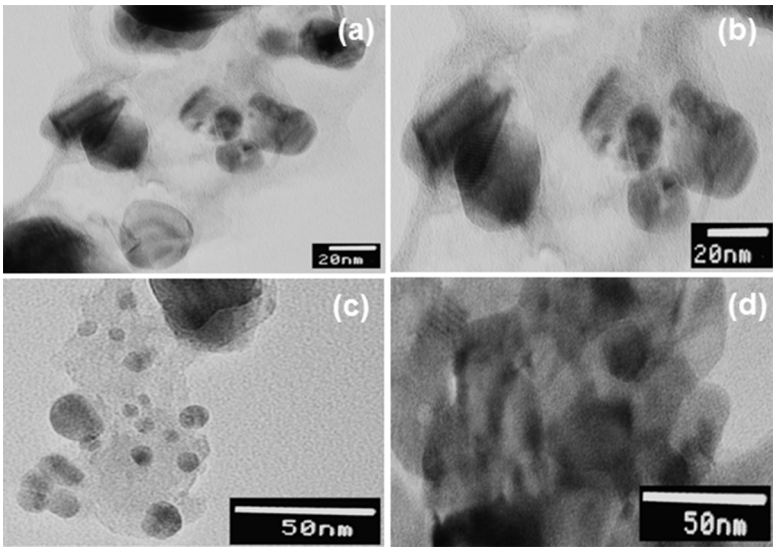

Fig. 6. TEM images of CMC/SiO_2 hybrids doped with a silver content of – 0.5 wt% (a and b) and 1.5 wt% (c and d) at different magnifications.

Ag (Fig. 6a and b). The images show that the silver nanoparticles (in the sample with higher concentration of Ag) aggregate to form clusters with different orientation between lattice fringes having a *d*-spacing of 0.2–0.25 nm corresponding to refraction [1 0 2] according to data base JCPDS [01-087-0598].

The antimicrobial activities of the investigated hybrid materials were tested with *B. subtilis* and *E. coli* K12 in batch experiment, measuring turbidity and plate method as CFUs after strains exposure to the materials with different Ag concentrations. The bacterial growth was measured as optical density of the LB broth and the data showed typical bacterial growth curves in both control variants (Fig. 7). *B. subtilis* exposed to 1.5 wt% Ag showed a complete inhibition (Fig. 7a). 0.5 wt% Ag led to suppression of growth phases, the lag-phases is prolonged and logarithmic phases were reduced. The growth curves for *E. coli* K12 followed the same tendency, the high silver concentrations suppressed the growth of microorganisms and no growth was observed (Fig. 7b). The growth of *E. coli* K12 was affected in a similar manner, but the effect was less pronounced when compared to *B. subtilis*.

The inhibitory effect of hybrid materials was further confirmed by evaluation of CFU on agar plates (Fig. 8). 0.5 wt% Ag reduced growth of both strains on the plates, and no growth was observed at 1.5 wt% Ag by *B. subtilis* (Fig. 8d).

The reduction of bacterial growth reached 100% by *B. subtilis* in the presence of 1.5 wt% Ag, whereas the reduction of growth by *E. coli* K12 was 95% (Table 1). 0.5 wt% Ag also affected bacterial growth – 75% by *B. subtilis* and 53% by *E. coli* K12. In batch experiments as indirect method, our results demonstrated no growth phases by both used microorganisms by 1.5% Ag. In the same time by plate method as a direct method, we observed 95% reduction of *E. coli*. The less pronounced effect on *E. coli* K12 is probably due to the different cell wall structure of Gram-positive and Gram-negative bacteria. Gram-positive *B. subtilis* is more sensitive to silver, than Gram-negative *E. coli*. Based on these results, the obtained hybrid materials with AgNps even with 0.5 wt% Ag have efficient antibacterial properties for both Gram-positive and Gram-negative bacteria.

The antibacterial action of silver may be due to the interaction with the bacterial cell wall resulting in cell wall rupture, leading to protein denaturation and cell death. Silver and silver ions can cause oxidative stress by free radical formation in cytoplasm and disruption of bacterial membrane. Many authors established that the action of silver nanoparticles is similar to that of silver ions (Rastogi et al., 2011). Yoon, Byeon, Park, & Hwang (2007) investigated the antibacterial activity of silver nanoparticles and reported that the *B. subtilis* is more sensitive to silver nanoparticles compared to *E. coli*, due to different cell wall structure of Gram-positive

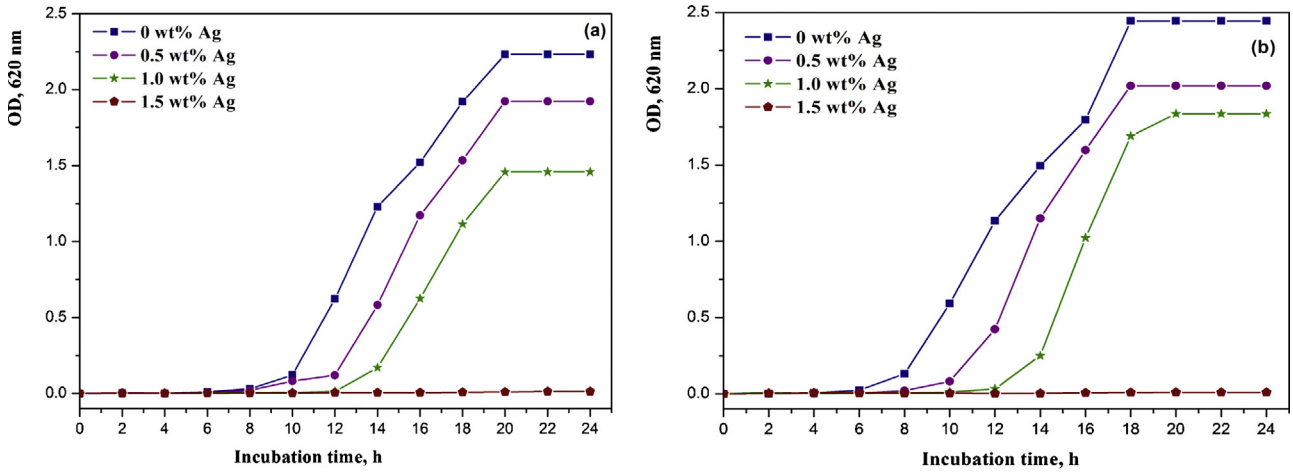

Fig. 7. Bacterial growth curves for *B. subtilis* (a) and *E. coli* K12 (b) in the presence of hybrid materials with different Ag contents.

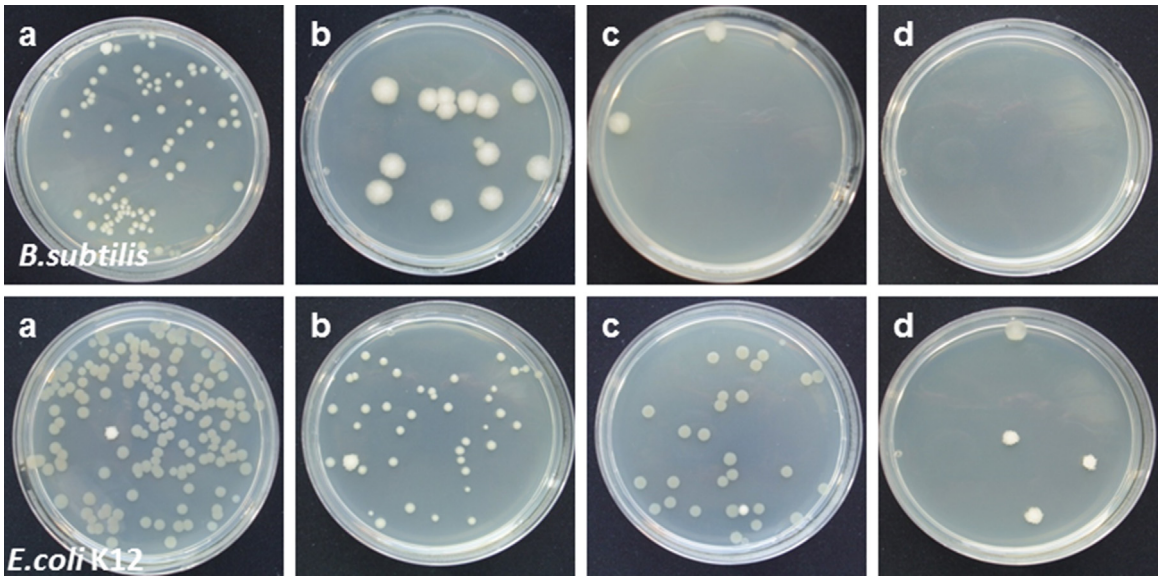

Fig. 8. Test results of *B. subtilis* (upper panel) and *E. coli* K12 (lower panel) cultivated on solid LB after 24 h: without Ag (a), in the presence of 0.5 wt% Ag (b), 1 wt% Ag (c) and 1.5 wt% Ag (d).

Table 1
Results of the tests on antibacterial activity of the hybrid materials.

SiO_2/CMC hybrid materials	*B. subtilis*		*E. coli K12*	
	CFU/ml	Reduction of bacteria (%)	CFU/ml	Reduction of bacteria (%)
0 wt % Ag	3.2×10^4	–	5×10^5	–
0.5 wt% Ag	0.8×10^4	75	2.35×10^5	53
1.0 wt% Ag	0.2×10^4	93.75	1.55×10^5	79
1.5 wt% Ag	–	100	0.25×10^5	95

and Gram-negative bacteria. Similar data were reported by Lara, Ayala-Nunez, Turrent, & Padilla (2010) as a result of investigation of bactericidal effect of silver nanoparticles against multidrug-resistant bacteria. They established that lipopolysaccharide might trap and block the positive charges of silver nanoparticles and make Gram-negative bacteria less sensitive to them. Our results also revealed greater sensitivity of *B. subtilis* compared to *E. coli*.

The mechanism of silver nanoparticles toxicity is complicated and depends on some factors such as their shape and size. It was demonstrated that truncated triangular silver displayed the strongest antibacterial action, compared to spherical and rod-like nanoparticles (Pal, Tak, & Song, 2007). The silver nanoparticles with a diameter of 1–10 nm attached to the surface of cell membrane and after penetrating inside the bacteria caused damage to the DNA (Morones et al., 2005). In our case the sample contain 1.5 wt% Ag shows the presence of irregularly shape with different size (5–10 nm) as compared to the hybrids with 0.5 wt% Ag where the size of obtained spherical silver nanoparticles is more than 20 nm. These results are confirmed also from the optical transmission spectra.

The applications of these materials can be in various fields such as improving water quality, medical devices and antimicrobial systems are possible.

4. Conclusions

A series of new silver doped SiO_2/CMC amorphous hybrid materials have been prepared. According to structural analysis it was proposed that the most probable mechanism of interaction between organic and inorganic components is the formation of new hydrogen bonds. These bonds are thermally more stable than the structure of macromolecules. It is suggested that the silver ions in the hybrids are present in different sizes and valence states (Ag^+ and Ag^0) in different ratios depending on the composition. The hybrids showed enhanced bactericidal activity against both Gram-positive (*B. subtilis*) and Gram-negative (*E. coli* K12) bacteria.

Acknowledgements

This work was supported by the National Science Fund (Ministry of Education of Bulgaria) Grant DDVU 02–96/20.12.2010. The help of Farhad Riazi (Hamburg University of Technology) with scanning electron microscopy is gratefully acknowledged.

References

Abdel-Halim, E. S., & Al-Deyab, S. S. (2011). Utilization of hydroxypropyl cellulose for green and efficient synthesis of silver nanoparticles. *Carbohydrate Polymers, 86*, 1615–1622.

Abdel-Mohsen, A. M., Hrdina, R., Burgert, L., Krylová, G., Abdel-Rahman, R. M., Krejcová, A., et al. (2012). Green synthesis of hyaluronan fibers with silver nanoparticles. *Carbohydrate Polymers, 89*, 411–422.

Ahmad, M. B., Shameli, K., Darroudi, M., Yunus, W. M. Z. W., & Ibrahim, N. A. (2009). Synthesis and characterization of silver/clay/chitosan bionanocomposites by UV irradiation method. *American Journal of Applied Sciences, 6*, 2030–2035.

Amin, M., Anwar, F., Janjua, M. R. S. A., Iqbal, M. A., & Rashid, U. (2012). Green synthesis of silver nanoparticles through reduction with *Solanum xanthocarpum* L. berry extract: Characterization, antimicrobial and urease inhibitory activities against *Helicobacter pylori*. *International Journal of Molecular Sciences, 13*, 9923–9941.

Angelova, Ts., Rangelova, N., Yuryev, R., Georgieva, N., & Müller, R. (2012). Antibacterial activity of SiO_2/hydroxypropyl cellulose hybrid materials containing silver nano particles. *Materials Science and Engineering C, 32*, 1241–1246.

Arreche, R. A., Blanco, M. N., Martín Martínez, J. M., & Vázquez, P. G. (2012). Structural synthesis of hydrophilic and hydrophobic silica for its use in food packaging films. *Procedia Materials Science, 1*, 572–579.

Aziz, S. B., Abidin, Z. H. Z., & Arof, A. K. (2010). Influence of silver ion reduction on electrical modulus parameters of solid polymer electrolyte based on chitosan–silver triflate electrolyte membrane. *eXPRESS Polymer Letters*, *4*, 300–310.

Baia, L., & Simon, S. (2007). UV–vis and TEM assessment of morphological features of silver nanoparticles from phosphate glass matrices. In A. Mendez-Vilas, & J. Diaz (Eds.), *Modern research and educational topics in microscopy* (pp. 576–583). Spain: Formatex.

Bankura, K. P., Maity, D., Mollick, M. M. R., Mondal, D., Bhowmick, B., Bain, M. K., et al. (2012). Synthesis, characterization and antimicrobial activity of dextran stabilized silver nanoparticles in aqueous medium. *Carbohydrate Polymers*, *89*, 1159–1165.

Benmouhoub, N., Simmonet, N., Agoudjil, N., & Coradin, T. (2008). Aqueous sol–gel routes to bio-composite capsules and gels. *Green Chemistry*, *10*, 957–964.

Chang, C., Duan, B., Cai, J., & Zhang, L. (2010). Superabsorbent hydrogels based on cellulose for smart swelling and controllable delivery. *European Polymer Journal*, *46*, 92–100.

Chen, J., Wang, J., Zhang, X., & Jin, Y. (2008). Microwave-assisted green synthesis of silver nanoparticles by carboxymethyl cellulose sodium and silver nitrate. *Materials Chemistry and Physics*, *108*, 421–424.

Dastjerdi, R., Montazer, M., & Shahsavan, S. (2010). Size-controlled preparation of silver nanoparticles by a modified polyol method. *Colloids and Surfaces A: Physicochemical and Engineering Aspects*, *366*, 197–202.

Du, W. L., Niu, S. S., Xu, Y. L., Xu, Z. R., & Fan, C. L. (2009). Antibacterial activity of chitosan tripolyphosphate nanoparticles loaded with various metal ions. *Carbohydrate Polymers*, *75*, 385–389.

Feller, R. L., & Wilt, M. (1990). *Evaluation of cellulose ethers for conservation*. J. Paul Getty Trust Printed in the United States of America.

García-Barrasa, J., López-de-Luzuriaga, J. M., & Monge, M. (2011). Silver nanoparticles: Synthesis through chemical methods in solution and biomedical applications. *Central European Journal of Chemistry*, *9*, 7–19.

Ghaffari, A., Navaee, K., Oskoui, M., Bayati, K., & Rafiee-Tehrani, M. (2007). Preparation and characterization of free mixed-film of pectin/chitosan/Eudragit® RS intended for sigmoidal drug delivery. *European Journal of Pharmaceutics and Biopharmaceutics*, *67*, 175–186.

Han, Y. H., Taylor, A., Mantle, M., & Knowles, K. (2007). Sol–gel derived organic–inorganic hybrid materials. *Journal of Non-Crystalline Solids*, *353*, 313–320.

Hatakeyama, T., & Hatakeyama, H. (2004). *Thermal properties of green polymers and biocomposites*. Dordrecht: Kluwer Academic Publishers.

Hebeish, A., Hashem, M., El-Hady, M. M. A., & Sharaf, S. (2013). Development of CMC hydrogels loaded with silver nano-particles for medical applications. *Carbohydrate Polymers*, *92*, 407–413.

Hebeish, A. A., El-Rafie, M. H., Abdel-Mohdy, F. A., Abdel-Halim, E. S., & Emam, H. E. (2010). Carboxymethyl cellulose for green synthesis and stabilization of silver nanoparticles. *Carbohydrate Polymers*, *82*, 933–941.

Husein, M., & Nassar, N. (2008). Nanoparticle preparation using the single microemulsions scheme. *Current Nanoscience*, *4*, 370–380.

Ibrahim, M. M., Koschella, A., Kadry, G., & Heinze, T. (2013). Evaluation of cellulose and carboxymethyl cellulose/poly(vinyl alcohol) membranes. *Carbohydrate Polymers*, *95*, 414–420.

Jeon, H.-J., Yi, S-Ch., & Oh, S.-G. (2003). Preparation and antibacterial effects of Ag–SiO_2 thin films by sol–gel method. *Biomaterials*, *24*, 4921–4928.

Jiang, H., Zuo, Y., Cheng, L., Wang, H., Gu, A., & Li, Y. (2011). A homogenous CS/NaCMC/n-HA polyelectrolyte complex membrane prepared by gradual electrostatic assembling. *Journal of Materials Science: Materials in Medicine*, *22*, 289–297.

Juby, A. K., Dwivedi, Ch., Kumar, M., Kota, S., Misra, H. S., & Bajaj, P. N. (2012). Silver nanoparticles-loaded PVA/gum acacia hydrogel: Synthesis, characterization and antibacterial study. *Carbohydrate Polymers*, *89*, 906–913.

Kang, S. W., Kim, J. H., Oh, K. S., Won, J., Char, K., Kim, H. S., et al. (2004). Highly stabilized silver polymer electrolytes and their application to facilitated olefin transport membranes. *Journal of Membrane Science*, *236*, 163–169.

Kapoor, S., Lawless, D., Kennepohl, P., Meisel, D., & Serpone, N. (1994). Reduction and aggregation of silver ions in aqueous gelatin solutions. *Langmuir*, *10*, 3018–3022.

Khan, Z., Al-Thabaiti, S. A., Obaid, A. Y., & Al-Youbi, A. O. (2011). Preparation and characterization of silver nanoparticles by chemical reduction method. *Colloids and Surfaces B: Biointerfaces*, *82*, 513–517.

Kheybari, S., Samadi, N., Hosseini, S. V., Fazeli, A., & Fazeli, M. R. (2010). Synthesis and antimicrobial effects of silver nanoparticles produced by chemical reduction method. *DARU Journal of Pharmaceutical Sciences*, *18*, 168–172.

Kickelbick, G. (2007). Introduction to hybrid materials. In G. Kickelbick (Ed.), *Hybrid materials: Synthesis, characterization, and applications* (pp. 1–46). Weinheim: WILEY-VCH Verlag GmbH & Co. KGaA.

Kim, H. S., Lee, K. H., & Kim, S. G. (2006). Growth of monodisperse silver nanoparticles in polymer matrix by spray pyrolysis. *Aerosol Science and Technology*, *40*, 536–544.

Kim, J. (2007). Thermal characteristics and degradation kinetics of cross-linked carboxymethyl cellulose sodium salt. *Electronic Journal of Environmental, Agricultural and Food Chemistry*, *6*, 2458–2472.

Kim, J. M., Chang, S. M., Kong, S. M., Kim, K.-S., Kim, J., & Kim, W.-S. (2009). Control of hydroxyl group content in silica particle synthesized by the sol-precipitation process. *Ceramics International*, *35*, 1015–1019.

Lara, H., Ayala-Nunez, N., Turrent, L., & Padilla, C. R. (2010). Bactericidal effect of silver nanoparticles against multidrug-resistant bacteria. *World Journal of Microbiology and Biotechnology*, *26*, 615–621.

Li, S.-M., Jia, N., Ma, M.-G., Zhang, Z., Liu, Q.-H., & Sun, R.-C. (2011). Cellulose–silver nanocomposites: Microwave-assisted synthesis, characterization, their thermal stability, and antimicrobial property. *Carbohydrate Polymers*, *86*, 441–447.

Li, S.-M., Jia, N., Zhu, J.-F., Ma, M.-G., Xu, F., Wang, B., et al. (2011). Rapid microwave-assisted preparation and characterization of cellulose–silver nanocomposites. *Carbohydrate Polymers*, *83*, 422–429.

Li, W., Sun, B., & Wu, P. (2009). Study on hydrogen bonds of carboxymethyl cellulose sodium film with two-dimensional correlation infrared spectroscopy. *Carbohydrate Polymers*, *78*, 454–461.

Li, Z., Shi, T., & Guo, L. (2010). Preparation and morphology of porous SiO_2 ceramics derived from fir flour templates. *Journal of the Serbian Chemical Society*, *75*, 385–394.

Lin, S., Huang, R., Cheng, Y., Liu, J., Lau, B. L. T., & Wiesner, M. R. (2013). Silver nanoparticle–alginate composite beads for point-of-use drinking water disinfection. *Water Research*, *47*, 3959–3965. http://dx.doi.org/10.1016/j.watres.2012.09.005

Liu, H., Huang, S., Li, X., Zhang, L., Tan, Y., Wei, C., et al. (2013). Facile fabrication of novel polyhedral oligomeric silsesquioxane/carboxymethyl cellulose hybrid hydrogel based on supermolecular interactions. *Materials Letters*, *90*, 142–144.

Maity, D., Mollick, Md. M. R., Mondal, D., Bhowmick, B., Bain, M. K., Bankura, K., et al. (2012). Synthesis of methylcellulose–silver nanocomposite and investigation of mechanical and antimicrobial properties. *Carbohydrate Polymers*, *90*, 1818–1825.

Mohan, Y. M., Raju, K. M., Sambasivudu, K., Singh, S., & Sreedhar, B. (2007). Preparation of acacia-stabilized silver nanoparticles: A green approach. *Journal of Applied Polymer Science*, *106*, 3375–3381.

Morones, J. R., Elechiguerra, J. L., Camacho, A., Holt, K., Kouri, J. B., Ramirez, J. T., et al. (2005). The bactericidal effect of silver nanoparticles. *Nanotechnology*, *16*, 2346–2353.

Moura, M. R., de Mattoso, L. H. C., & Zucolotto, V. (2012). Development of cellulose-based bactericidal nanocomposites containing silver nanoparticles and their use as active food packaging. *Journal of Food Engineering*, *109*, 520–524.

Nenkova, S., Radev, L., Rangelova, N., Aleksiev, B., & Samuneva, B. (2007). New sol-gel silica hybrids containing pectin and some metal ions. *Physics and Chemistry of Glasses – European Journal of Glass Science and Technology, Part B*, *48*, 164–167.

Pal, S., Tak, Y. K., & Song, J. M. (2007). Does the antibacterial activity of silver nanoparticles depend on the shape of the nanoparticle? A study of the Gram-negative bacterium *Escherichia coli*. *Applied and Environmental Microbiology*, *73*, 1712–1720.

Pandey, S., Goswami, G. K., & Nanda, K. K. (2012). Green synthesis of biopolymer–silver nanoparticle nanocomposite: An optical sensor for ammonia detection. *International Journal of Biological Macromolecules*, *51*, 583–589.

Pourjavadi, A., & Soleyman, R. (2011). Silver nanoparticles with gelatin nanoshells: Photochemical facile green synthesis and their antimicrobial activity. *Journal of Nanoparticle Research*, *13*, 4647–4658.

Rangelova, N. (2012). University of Chemical Technology and Metallurgy, in Sofia, Bulgaria. *PhD thesis, Preparation, characterization and application of biopolymer/SiO2 hybrid materials, Scientific Supervisors: Prof. D. Sc. Sanchi Nenkova and Prof. Dr. Biserka Samuneva*.

Rangelova, N., Georgieva, N., Mileva, K., Yuryev, R., & Müller, R. (2012). Synthesis and antibacterial activity of SiO_2–CMC–Ag hybrid materials prepared by sol–gel method. *Comptesrendus de l'Academie bulgare des Science*, *65*, 1057–1064.

Rangelova, N., Nenkova, S., Chernev, G., Georgieva, N., Yotova, L., Salvado, I., et al. (2010). Synthesis, characterization and application of SiO_2–methylcellulose hybrid materials. In E. Balabanova, & I. Dragieva (Eds.), *Nanoscience and nanotechnology* (vol. 10) (pp. 172–174). Sofia: Heron Press.

Rangelova, N., Nenkova, S., Radev, L., Samuneva, B., & Aleksiev, B. (2007). Sol–gel synthesis and structure of silica hybrids containing low methoxyl pectin. In E. Balabanova, & I. Dragieva (Eds.), *Nanoscience and nanotechnology* (7) (pp. 230–234). Sofia: Heron Press.

Rangelova, N., Radev, L., Nenkova, S., Salvado, I. M., Fernandes, M. H., & Herzog, M. (2011). Methylcellulose/SiO_2 hybrids: Sol–gel preparation and characterization by XRD, FTIR and AFM. *Central European Journal of Chemistry*, *9*, 112–118.

Rastogi, Sh., Rutledge, V., Gibson, Ch., Newcombe, D., Branen, J., & Branen, L. (2011). Ag colloids and Ag clusters over EDAPTMS-coated silica nanoparticles: Synthesis, characterization and antibacterial activity against *Escherichia coli*. *Nanomedicine: Nanotechnology, Biology and Medicine*, *7*, 305–314.

Rivero, P. J., Urrutia, A., Goicoechea, J., Zamarreño, C. R., Arregui, F. J., & Matías, I. R. (2011). An antibacterial coating based on a polymer/sol–gel hybrid matrix loaded with silver nanoparticles. *Nanoscale Research Letters*, *6*, 305–311.

Savage, N., & Diallo, M. S. (2005). Determination of ascorbic acid by modified method based on photoluminescence of silver nanoparticles. *Journal of Nanoparticle Research*, *7*, 331–342.

Setua, P., Chakraborty, A., Seth, D., Bhatta, M. U., Satyam, P. V., & Sarkar, N. (2007). Glucosamine-functionalized silver glyconanoparticles: Characterization and antibacterial activity. *Journal of Physical Chemistry C*, *111*, 3901–3907.

Sharma, V. K., Yngard, R. A., & Lin, Y. (2009). Silver nanoparticles: Green synthesis and their antimicrobial activities. *Advances in Colloid and Interface Science*, *145*, 83–96.

Shchipunov, Y. A. (2008). Entrapment of biopolymers into sol–gel-derived silica nanocomposites. In E. Ruiz-Hitzky, K. Ariga, & Yu. Lvov (Eds.), *Bio-inorganic hybrid nanomaterials* (pp. 75–103). Weinheim: WILEY-VCH Verlag GmbH & Co. KGaA.

Shi, Q., Vitchuli, N., Nowak, J., Caldwell, J. M., Breidt, F., Bourham, M., et al. (2011). Durable antibacterial Ag/polyacrylonitrile (Ag/PAN) hybrid nanofibers prepared

by atmospheric plasma treatment and electrospinning. *European Polymer Journal*, *47*, 1402–1409.

Silvert, P.-Y., Herrera-Urbina, R., & Tekaia-Elhsissen, K. (1997). Preparation of colloidal silver dispersions by polyol process. *Journal of Materials Chemistry*, *7*, 293–299.

Singh, V., & Ahmed, Sh. (2012a). Silver nanoparticles (AgNPs) doped gum acacia–gelatin–silica hybrid: An effective support for diastase immobilization. *International Journal of Biological Macromolecules*, *50*, 353–361.

Singh, V., & Ahmed, Sh. (2012b). Synthesis and characterization of carboxymethyl cellulose–silver nanoparticle (AgNp)-silica hybrid for amylase immobilization. *Cellulose*, *19*, 1759–1769.

Tao, A., Sinsermsuksaku, P., & Yang, P. (2006). Polyhedral silver nanocrystals with distinct scattering. *Angewandte Chemie International Edition*, *45*, 4597–4601.

Vasireddy, R., Paul, R., & Mitra, A. K. (2012). Green synthesis of silver nanoparticles and the study of optical properties. *Nanomaterials and Nanotechnology*, *2*, 1–6.

Vulpoi, A. (2011). Babes-Bolyai University, in Cluj-Napoca, Romania. *PhD thesis, Studies on composite biomaterials, Scientific Supervisor: Prof. Dr. Viorica Simon*.

Wang, J., & Somasundaran, P. (2005). Adsorption and conformation of carboxymethyl cellulose at solid–liquid interfaces using spectroscopic, AFM and allied techniques. *Journal of Colloid and Interface Science*, *291*, 75–83.

Wang, L., & Xu, Y. (2006). Preparation and characterization of graft copolymerization of ethylacrylate onto hydroxypropylmethyl cellulose in aqueous medium. *Cellulose*, *13*, 191–200.

Wiley, B., Sun, Y., Mayers, B., & Xi, Y. (2005). Shape-controlled synthesis of metal nanostructures: The case of silver. *Chemistry – A European Journal*, *11*, 454–463. Commonly used reductants are borohydride, citrate, ascorbate, and elemental hydrogen (15–17) (2005).

Yang, F., Li, G., He, Y.-G., Ren, F.-X., & Wang, G.-X. (2009). Synthesis, characterization, and applied properties of carboxymethyl cellulose and polyacrylamide graft copolymer. *Carbohydrate Polymers*, *78*, 95–99.

Yang, G., Xie, J., Deng, Y., Bian, Y., & Hong, F. (2012). Hydrothermal synthesis of bacterial cellulose/AgNPs composite: A "green" route for antibacterial application. *Carbohydrate Polymers*, *87*, 2482–2487.

Yano, S. (1994). Preparation and characterization of hydroxypropyl cellulose/silica micro-hybrids. *Polymer*, *35*, 5565–5570.

Yoon, K., Byeon, J. H., Park, J., & Hwang, J. (2007). Susceptibility constants of *Escherichia coli* and *Bacillus subtilis* to silver and copper nanoparticles. *Science of the Total Environment*, *373*, 572–575.

Yugang, S., Mayers, B., & Xia, Y. (2003). Polyol synthesis of uniform silver nanowires: A plausible growth mechanism and the supporting evidence. *Nano Letters*, *3*, 955–960.

Zakharov, H. A., Ezhova, A. Zh., Koval, E. M., Kalinnikov, V. T., & Chalykh, A. E. (2005). Hydroxyapatite–carboxymethyl cellulose nanocomposite biomaterials. *Inorganic Materials*, *41*, 592–599.

Zhang, X., Wu, Y., He, S., & Yang, D. (2007). Structural characterization of sol–gel composites using TEOS/MEMO as precursors. *Surface and Coatings Technology*, *201*, 6051–6058.

Teotia, A. (2012). Modification of carboxymetyl cellulose through oxidation. *Carbohydrate Polymers*, *87*, 457–460.